INTERNATIONAL JOURNAL OF
COASTAL & OFFSHORE ENGINEERING IJCOE Vol.6/No.5 /Autumn 2021 (39-50)/ **Special issue of "Marine Renewable Energy"**

Available online at: www. Ijcoe.org

The Application of Energy Absorbers to Harness Wave Energy in the Caspian Sea: A Feasibility Study

Mohammad Hossein Jahangir [1*], Mehran Mazinani [2], Zahra Ranji[3]

[1*] *Associated Professor, Faculty of New Sciences and Technologies, University of Tehran, Iran; mh.jahangir@ut.ac.ir*
[2] *MSc. Student, Faculty of New Sciences and Technologies, University of Tehran, , Iran; mzn.mehran@gmail.com*
[3] *MSc. Student, Faculty of New Sciences and Technologies, University of Tehran, , Iran; zahra.ranji@ut.ac.ir*

ARTICLE INFO

Article History:
Received: 06 Feb. 2021
Accepted: 1 Sep. 2021

Keywords:
Wave Energy Converter
Energy Absorbers
Caspian Sea
Feasibility Study

ABSTRACT

Since renewable energy can be a good solution to respond to oil crises, the disadvantages of using them and increasing energy demand in a sustainable way in the future, and because the oceans cover two-thirds of the earth's surface, harnessing the energy of the oceans can be a source of green energy for coastal areas. At present, the generation of electricity from ocean waves by wave energy converters is considered as a potential future energy source in many countries. Currently, the electricity generation from ocean waves by wave energy converters is considered as a potential future energy source in many countries. Therefore this study aims to investigate the potential of wave energy in the Caspian Sea from the Iranian perspective, and in the next step, propose a framework to select an absorber to harvest this energy. Although there are studies to assess the potential of wave energy in this region,but none of them considered more than one type of absorber in the models. To this aim, the wind data samples of the European Center for Medium-Range Weather Forecasts are used to model the Caspian sea by implementing Mike 21 software from which the power and height of waves data are obtained within the years 2001 to 2015. Based on the results of this phase and the geographical conditions, a weighting framework is applied to select an absorber for harvesting wave energy. The results indicate that the best technology to harness energy in the Caspian Sea is the WEPTOS absorber. This technology benefits from low complexity while offering high efficiency.

1. Introduction

The oil crisis in the 1970s prompted the world to explore alternatives for fossil fuels [1]. Furthermore, it is expected that the world's energy demand will increase by 30 percent from 2010 to 2040 [2,3]. Renewable energies could be a solution to meet demand in a sustainable way in the future [4] and since the oceans cover two-thirds of the Earth's surface, harnessing ocean energy could be a green energy supply for coastal regions [5]. Currently, the electricity generation from ocean waves by wave energy converters (WECs) is considered as a potential future energy source in many countries [6,7]. Fluctuated power generation due to inherently fluctuations of renewables such as wind and solar electricity supplies could cause instability in energy systems. This instability comes from a mismatch between the electricity production pattern and electric load profile. Wave energy converters (WECs) can produce electricity from the waves with a lower rate of power fluctuation and higher capacity factor compared to wind and solar supplies, which have the capacity factors around 30% and 20%, respectively [8–11]. Moreover, the wave resources compared to other variable renewable resources generate energy with advantages including, predictability, availability, and less land acquisition [12–17]. Although numerous research regarding renewable energies utilization has been conducted in Iran, the wave energy harvesting has been studied the least. In this study, we intend to evaluate the Caspian sea shoreline wave energy potentials and to propose the most befitting wave energy converter (WEC) technology to harness this energy. Table 1 provides the details of these projects. [18].

Table 1. Specification of renewable energy projects of Iran

Renewable energy	Project name	Capacity of project (Mw)
Wind	111 installed turbines in Manjil	61.18
	43 installed turbines in Binalud	28.38
	4 installed turbines in Tabriz	0.67
Solar	Darbid Yazd and SarKavir Semnan Power plant development	0.012 – 0.017
	Solar water heater in Yazd, Khorasan, Sistan and Baluchestan and Isfahan	4.312
	Shiraz solar plant (Vapor phase)	0.25
Geothermal	Meshkinshahr geothermal power plant(Conduct exploration drilling, production and injection) in Ardabil	50
	Construction 3–5 MW package in Ardabil	3 - 5
Biomass and Biogass	Manufacture of semi-industrial stack	
	Vanadium redox battery in Alborz(Energy reservation)	0.001
	Feasibility study for installing of biomass power plant in Fars and Khorasan(Survey potential-land fill)	1.06 – 0.65
		1.2 – 0.66
	Construction biomass power plant in Shiraz and Mashhad(Land fill)	0.6
	Feasibility study for manufacturing of Biogas in Saveh	
Fuel cell and Hydrogen	Purchase, installation and operation of 25 kW fuel cell polymer and Accessories in Alborz	0.025
	Semi-industrial scale pilot projects in hydrogen technology in Alborz	0.2

Although the first wave energy converter (WEC) was created in 1799 in France by Gerard and his son, Masuda can be recognized as the father of the modern wave energy. He launched a navigation buoy equipped with an air turbine, which is now called the OWC converter. In recent years, the WEC technologies have improved and developed significantly [19–23]. Moreover, studies [24] tested the commercial size of WECs in the oceans to harvest energy from waves. The value of the wave energy hinges on the wavelength and wave height [25]. As a result, studies [26] in this field mostly focused on the aforementioned features to assess the energy characteristics of wave energy resources. Studies [25] investigated the potential of wave energy resources in the Caspian Sea, the Persian Gulf, and the Gulf of Oman and found a large number of hotspots with high energy potential Iran. Previous studies [27], with the same regions of study, proposed three districts in Iran (Qeshm, Chabahar, and Anzali) as the best candidate for deployment of wave energy stations using 3-h wind data from 2010. Other studies [28] found two districts in Iran, including Noshahr and Babolsar, as attractive locations to install wave energy converters. Studying 11-year wind data of the Caspian Sea using the (Simulation Wave Numerical) SWAN software [29] depicted that the central zone of this region has the highest wave energy potential while the northern zone has the lowest potential. In other studies [30], the same software, SWAN software, is used to model wave energy resources in the Gulf of Oman in the south of Iran, indicating 2.8 kW/m annual energy for this region. Studies found a range of 0.2 and 1.2 kW/m annual energy for the wave energy resources in the Caspian Sea (Anzali port coast), showing that the wave power is more considerable in winter and spring than summer and autumn.

The WECs are divided into four main categories: Wave Bodies Active (WAB) [31], Oscillating Water Column(OWC) [32], Point Absorbers [33] and Overtopping [34] that can be placed from the shore to the sea.

Although there are studies [35,36] to assess the potential of wave energy around the world, there is a gap in the scope of studies to fully investigate the different types of absorbers. In Iran, so far, no energy converters have been installed for capturing the energy of the Caspian Sea. Therefore, the aim of this study, initially, is to model the waves characteristics of this sea, and subsequently choose an energy converter system by evaluating the characteristics of the sea waves and examining the dynamic and geographical features of the Caspian Sea.

2. Model Description

Numerous software can be used to simulate and determine the wave energy. in the present study, MIKE software was selected and implemented. Initially, we model the waves of Caspian sea using the third generation of Mike 21 SW software. This version is one of the latest MIKE 21 software modules, replaced the OSW (Off Shore Wave) module. The SW model is a third-generation wavelength spectral model which is used to simulate the production, growth, decay and transformation of wind-generated waves and swell offshore and coastal areas [37]. The basic conservation equations are formulated in either Cartesian coordinate for a small-scale application. To generalize the governing equation in geographical and spectral space, the cell centered finite volume method is applied. An unstructured mesh technique is used in the geographical domain. The time integration is performed using a fractional step approach where a multi-sequence explicit is applied to the propagation of wave action.

The dynamics of the gravitational waves are described by the transport equation for wave action density. The wave action density spectrum is a function of two wave phase parameters (varies in time and space). The two wave phase parameters can be the wave direction, θ, and either the relative (intrinsic) angular frequency, or the absolute angular frequency. Alternatively, the wave phase parameters can be also the wave number vector, $\vec{k}$ with magnitude, k and direction, θ. The relative angular frequency, σ ,and the wave direction, θ., have been chosen to formulate the dynamics of the gravitational waves in the current model.
The action density relates to the energy density by:

$$N = \frac{E}{\sigma} \tag{1}$$

where in Eq.(1) N (σ, θ) and E (σ, θ) stand for action density and energy density, respectively.
For wave propagation over gradually varying depths and currents, the relation between the relative angular frequency and the absolute angular frequency, are described by the linear dispersion relation:

$$\sigma = \sqrt{gk\tanh(kd)} = \omega - \vec{k}.\vec{U} \tag{2}$$

Where in Eq.(2) g is the acceleration of gravity, d is the water depth, ω is absolute angular frequency, and $\vec{U}$ is the current velocity factor. The magnitude of the group velocity of the wave energy relative to the current, c_g, is described by:

$$c_g = \frac{\partial_\sigma}{\partial_k} = \frac{1}{2}\left(1 + \frac{2kd}{sinh(2kd)}\right)\frac{\sigma}{k} \tag{3}$$

Where in Eq.(3) c describes the phase velocity of the wave relative to the current follows:

$$c = \frac{\sigma}{k} \tag{4}$$

A range between a minimum frequency, σ_{min} limits the frequency spectrum which is split up into a deterministic prognostic part for frequencies lower than a cut-off frequency and analytical diagnostic part for frequencies higher than the cut-off frequency. Based on WAMDI Group (1988) and Komen et al. (1994), a dynamic cut-off frequency depending on the local wind speed and mean frequency is used as in the WAM Cycle 4 model.
The governing equation, based on Komen et al. (1994) and Young (1999), is defined as the wave action balance equation which has been formulated in either Cartesian of spherical coordinate.

2.1. Cartesian coordinates

The conservation equation for wave action, in horizontal Cartesian coordinate, can be describes as:

$$\frac{\partial N}{\partial t} + \nabla.(\vec{v}N) = \frac{S}{\sigma} \tag{5}$$

Where in Eq.(5) N($\vec{x}.\sigma.\theta.t$) depicts the action density and t shows the time, $\vec{x} = (x.y)$ is the Cartesian co-ordinates, S is the source term for the energy balance equation, and $\vec{v} = (c_x, c_y, c_\sigma, c_\theta)$ refers to the propagation velocity of a wave in the four-dimensional phase space $\vec{x}$, σ and θ. ∇ is the four-dimensional differential operator in the $\vec{x}$, σ, θ-space. The four characteristic propagation speeds are described by:

$$\left(c_x.c_y\right) = \frac{\overrightarrow{dx}}{dt} = \overrightarrow{c_g} + \vec{U} \tag{6}$$

$$c_\sigma = \frac{d\sigma}{dt} = \frac{\partial\sigma}{\partial d}\left[\frac{\partial d}{\partial t} + \vec{U}.\nabla_{\bar{x}}d\right] - c_g\vec{k}.\frac{\partial\vec{U}}{\partial s} \tag{7}$$

$$c_\theta = \frac{d\theta}{dt} = -\frac{1}{k}\left[\frac{\partial\sigma}{\partial d}\frac{\partial d}{\partial m} + \vec{k}.\frac{\partial\vec{U}}{\partial m}\right] \tag{8}$$

Where in Eq.(7) s represents the space coordinate in wave direction θ, and in Eq.(8) m is a coordinate perpendicular to s. $\nabla_{\bar{x}}$ Is the two-dimensional differential operator in the $\vec{x}$-space.

2.2. Spherical coordinates

The conserved property is spherical coordinates, is the action density $\hat{N}(\vec{x},\sigma,\theta,t)$. Here, $\vec{x}$= (ϕ,λ) is the spherical co-ordinates, where ϕ is the latitude and λ is the longitude. The action density $\hat{N}$ is related the normal action density N (and normal energy density E) while $\hat{N}d\sigma d\theta d\phi d\lambda = Nd\sigma d\theta dxdy$, or:

$$\hat{N} = NR^2\cos\phi = \frac{ER^2\cos\phi}{\sigma} \tag{9}$$

Where in Eq.(9) R shows the radius of the earth. The wave action balance equation in spherical polar coordinates is following:

$$\frac{\partial\hat{N}}{\partial t} + \frac{\partial}{\partial\phi}c_\phi\hat{N} + \frac{\partial}{\partial\lambda}c_\lambda\hat{N} + \frac{\partial}{\partial\sigma}c_\sigma\hat{N} + \frac{\partial}{\partial\theta}c_\theta\hat{N} = \frac{\hat{S}}{\sigma} \tag{10}$$

Here in Eq.(10) $\hat{S}(\vec{x},\sigma,\theta,t)$=S$R^2\cos\phi$ is the total source and sink function. S is the energy source term which depicts the superposition of source function describing various physical phenomena:

$$S = S_{in} + S_{nl} + S_{ds} + S_{bot} + S_{surf} \tag{11}$$

Here in Eq.(11) S_{in} represents the generation of energy by wind, S_{nl} is the wave energy transfer due to non-linear wave-wave interaction, S_{ds} is the dissipation of wave energy because of white-capping, S_{bot} is the dissipation because of bottom friction and S_{surf} is the dissipation of wave energy because of depth-induced breaking.

The spectral moment of order ith for the calculation of spectral wave parameters is computed by the equation in mike 21 SW model:

$$m_i = \int_0^{2\pi} \int_0^{\infty} E(f.\theta) f^i df d\theta \qquad (12)$$

Where in Eq.(12) E(f,θ) is the direct spectrum of wave energy and f is the wave frequency. Thus, the height characteristics of the wave Hs, the wave period Te and the mean period of time Tm are obtained from the following equations:

$$H_s = 4\sqrt{m_0}$$

$$T_e = \frac{m_{-1}}{m_0} \qquad (13)$$

$$T_m = \frac{m_0}{m_1}$$

The flux of energy per unit length, so-called wave power, P, is defined by equation (14):

$$P = \rho g \int_0^{2\pi} \int_0^{\infty} c_g(f.\theta) E(f.\theta) df\, d\theta \qquad (14)$$

Where in Eq.(14) ρ is the density of the seawater as follows. In deep water(d> $0.5L$) follows equation (15):

$$P = \frac{\rho g^2}{64\pi} H_s^2 T_e \approx (0.49) H_s^2 T_e \ \ kW/m \qquad (15)$$

2.3. Model setup

Data from monitoring wind for 6 hours at a distance of 10 meters from the ECMWF (European Center for Medium-Range Weather Forecasts) was used with a resolution of 0.75×0.75 square kilometers in order to model the sea waves. To validate this model, results are compared with the measured data of buoys on the Anzali coast with geographical coordinates of 49.52 degrees north and 37.55 degrees eastern within May 2003 to June 2003 as well as city of Neka with geographical coordinates of 51.51 degrees north and 37.87 degrees east from October 2006 to May 2007.

2.4. Model Validation

The model validation is done using the aforementioned parameters and periods. For a more accurate evaluation of the accuracy of the validation results, for each of the courses, the scatter results are plotted and the statistical parameters that represent the accuracy of the matching two series of data are presented. These parameters include: Model skill (Ia), Scattering Index (SI), Correlation Coefficient (CC), BIAS and Root Mean Square Errors (RMSE).

Each of the above parameters are described in the following statistical relationships where x is the statistical series for results of the measurements, y is the statistical series of the results of the mode, $\bar{x}$ and $\bar{y}$ are mean of each of these two series and n is the total number of data in the statistical series. The results of the final validation are described in detail in Table 2.

$$I_a = 1 - \frac{\sum (x_i - y_i)^2}{\sum \left(|x_i - \bar{x}| + |y_i - \bar{y}|\right)^2} \qquad (16)$$

$$SI = \frac{\sqrt{\frac{1}{n}\Sigma((y_i - \bar{y}) - (x_i - \bar{x}))^2}}{\bar{x}}$$

$$CC = \frac{\Sigma(x_i - \bar{x})(y_i - \bar{y})}{\sqrt{\Sigma(x_i - \bar{x})^2 \Sigma(y_i - \bar{y})^2}}$$

$$Bias = (\bar{y} - \bar{x})$$

$$RMSE = \sqrt{\frac{1}{n}\Sigma(y_i - x_i)^2}$$

Table 2. Summary of error values obtained at the Caspian Sea Validation Station

	H_s (m)				
	I_a	SI	CC	$BIAS(m)$	$RMSE(m)$
Anzali	0.89	0.89	0.82	0.11	0.33
Neka	0.93	0.45	0.89	0.15	0.37
	T_p (s)				
Anzali	0.79	0.34	0.76	0.86	1.38
Neka	0.89	0.21	0.79	0.01	1.11

As can be seen in Figures 1a and 1b for port of Anzali and Figures 2a and 2b for port of Neka as well as Table 2, the modeling results show a good fit based on the measurement values in the mentioned time periods. Thus, the modeling of the Caspian Sea for 15 years from 2001 to 2015 is performed using the proposed model.

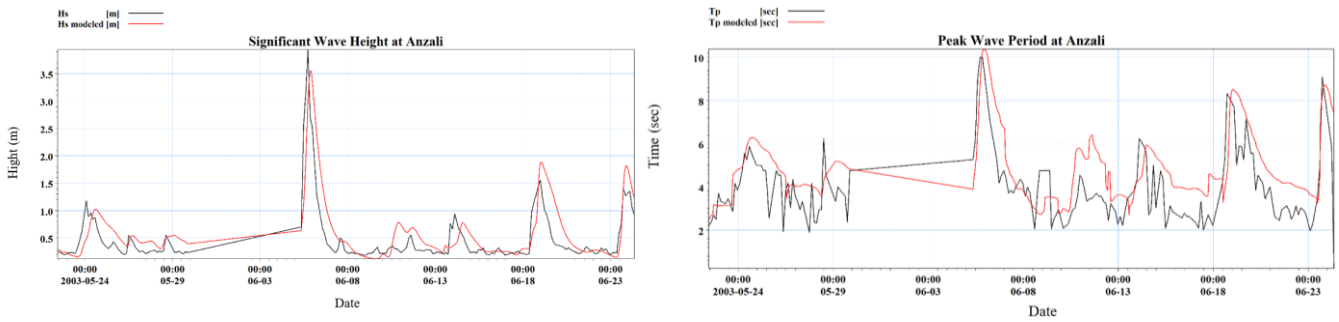

Figure 1. wave characteristics of port of Anzali in 2003

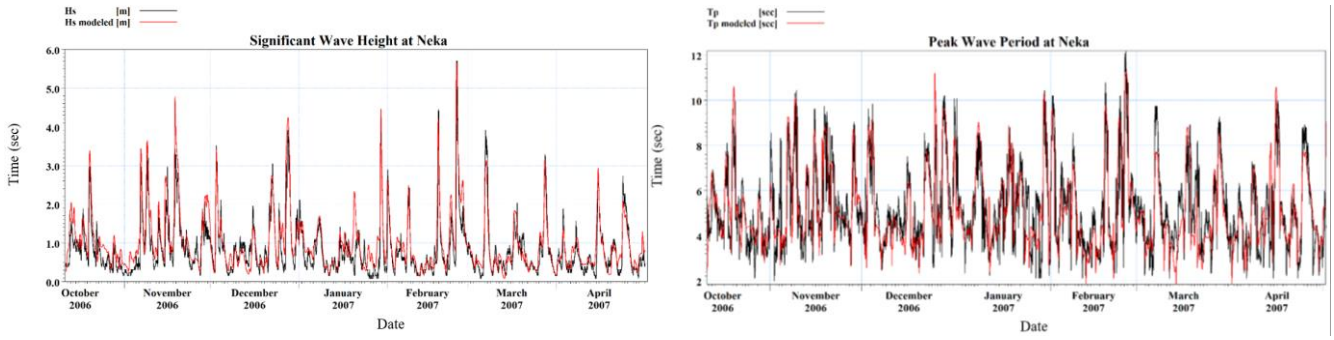

Figure 2. wave characteristics of port of Neka in 2003

3. The simulation of the Caspian Sea waves

3.1. Caspian Sea Wave

In this section, we provide details about modeling Caspian Sea for 15 years (from 2001 to 2015). Figure 3 shows the location of the Caspian Sea which is located between the 47.13 and 36.34 latitudes and 46.43 and 54.51 longitudes. The Caspian Sea ,with 7000 km shoreline, is the largest lake around the world surrounded by Iran in the south, Kazakhstan and Turkmenistan in the east and Russia in the north and North West and Azerbaijan in the west.

Figure 3. Location of Caspian Sea

The associated counter related to the wave heights in 2015 is shown in Figure 4 and Figure 5. As it can be seen, due to the low wind speeds in the spring, the average wave height is about 1 meter in the first season of the year for April to May months. Though, with the arrival of the summer season, due to the high temperature variation within day and night, the wind Speed has increased and the average wave height increased slightly and reached about 2 meters, around twice that of the spring. In the autumn, the wave height values in the Caspian Sea peak, and this amount decreases slightly in winter, but with thesecontours, it can be seen that the highest wave height values occur in the autumn and winter seasons.

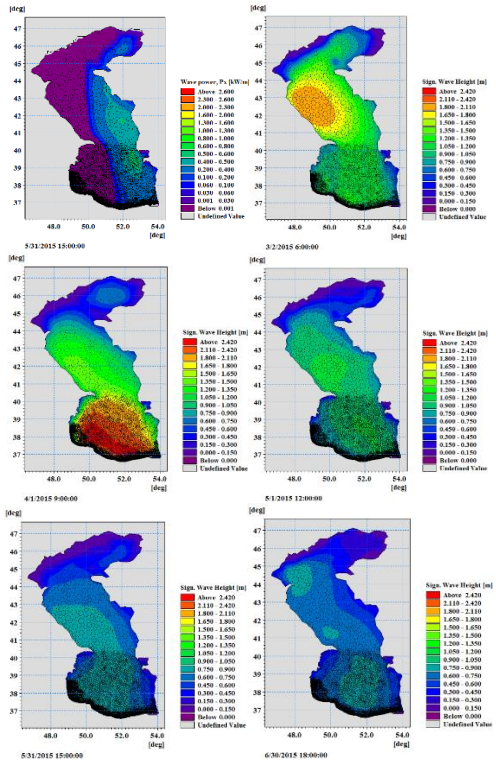

Figure 4. Counter of the Caspian Sea wave peaks in the first half of the year

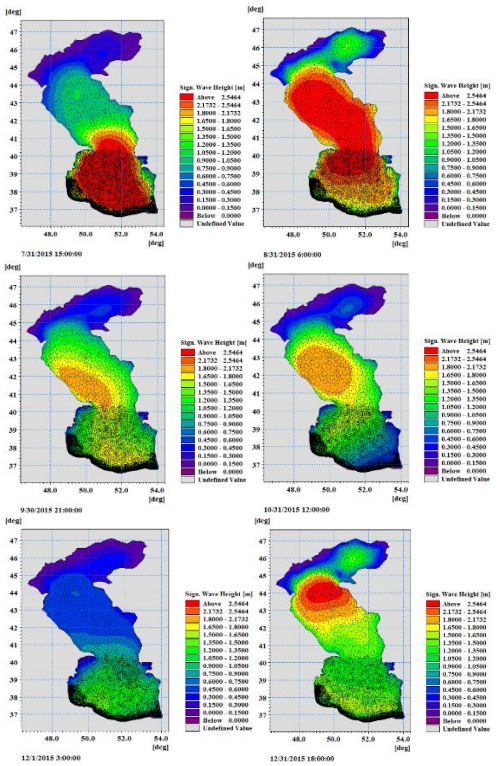

Figure 5. Counter of the Caspian Sea wave peaks in the second half of the year

Figure 6 depicts the locations which has been chosen for further investigation on the southern coast of the Caspian Sea. The main criteria for choosing these points is their importance based on harbor activities. Therefore, in commercial or fishery ports, the results of modeling and statistical analysis are presented with higher accuracy than the other points. These 23 stations are represents of the region of the case study which are described in Table 3.

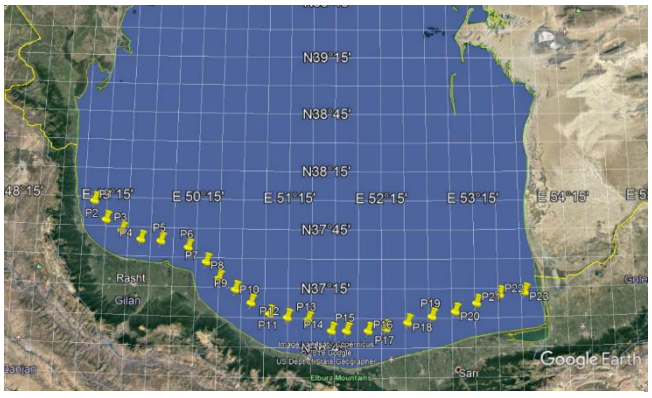

Figure 6. Location of the Chosen Stations

Table 3. The characteristics of the selected wave stations

Selected point	Coordinates (Lon/Lat)(°)	Water depth(m)	Closest urban centers
P1			
P2			
P3	49.09 N, 37.90 E	-15.5	Talesh
P4	49.23 N, 37.74 E	-26	Paresar
P5	49.41 N, 37.65 E	-56	Sangachin
P6	49.62 N, 37.58 E	-235	Hassanroud
P7	49.84 N, 37.57 E	-287	Hagi Bekandeh
P8	50.14 N, 37.52 E	-272	Mohsen Abad
P9	50.34 N, 37.40 E	-250	Amirabad
P10	50.48 N, 37.26 E	-366	Rudsar
P11	50.66 N, 37.17 E	-380	Oshiyan
P12	50.83 N, 37.06 E	-349	Ramsar
P13	51.03 N, 36.97 E	-471	Tonekabon
P12	51.22 N, 36.94 E	-551	Nashtarud
P13	51.44 N, 36.92 E	-584	Namakabrud
P12	51.69 N, 36.83 E	-499	Nowshahr
P13	51.85 N, 36.83 E	-488	Tooskatok
P14	52.08 N, 36.83 E	-467	Nur
P15	52.27 N, 36.85 E	-379	Mahmudabad
P16	52.50 N, 36.90 E	-392	Sorkhroud
P17	52.76 N, 36.95 E	-213	Babolsar
P18	53.01 N, 36.99 E	-176	Khazarabad
P19	53.24 N, 37.06 E	-95	Zeynaroud
P20	53.49 N, 37.13 E	-21	Emamadeh
P21	53.76 N, 37.15 E	-10	Bandar Torkaman
P22			
P23			

The result of the modeling is presented as wave characteristics and wave roses graphs. The simulation was performed for the selected stations and the mean results for fifteen years were presented in Figure 7. As it can be seen in this Figure, the selected stations P6 to P19 have the highest amount of wave power in the central-southern side of the Caspian sea which makes them suitable locations to harness wave energy. This potential wave energy in the west-southern and east-southern sides is lower compared to the central side (the eastern side has the lowest wave power potential). In the spring, due to low-speed wind blowing in the Caspian Sea, the wave power reaches its minimum (see Figure 7 (a)). This power increases in the summer by raising the wind speed and then reaches its highest value in the autumn. The wave power in the winter and autumn is almost twice the power in the summer and spring for the region of the case study (see Figure 7).

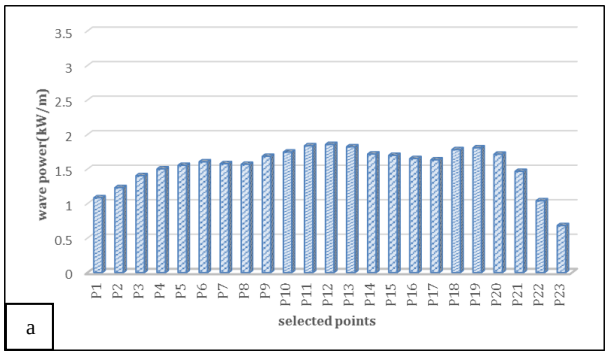

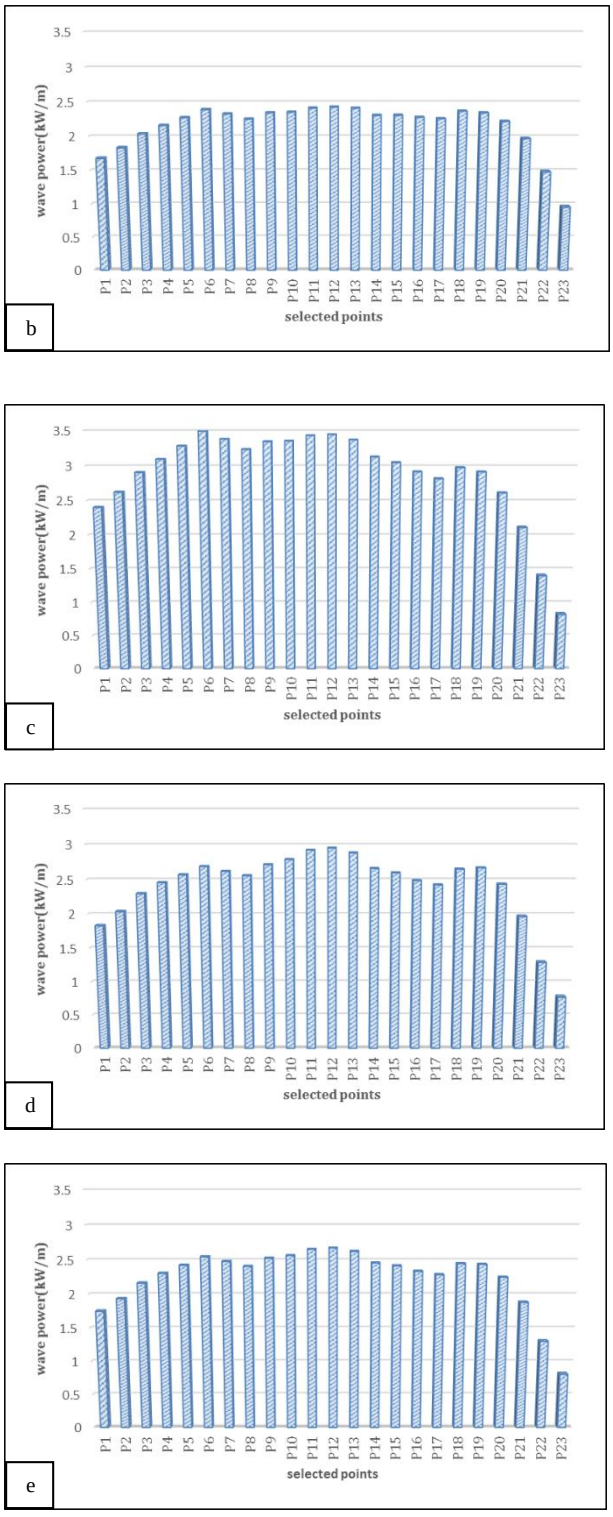

Figure 7. The measured mean wave power within the 15 years period for the selected stations in: (a) spring, (b) summer, (c) autumn, (d) winter and (e) annual

Figure 8 represents the wave rose, wind rose and power rose charts of the selected stations during the period of 15 years. Each unit in the x and y axis correlate to 10% of the total surface. The efficiency of the WECs highly hinges on the wave direction which should be consider in the installation procedure. The simulation results show that the direction of the waves, on the southern coast of the Caspian Sea, is towards north-east for the west side, towards the north in the middle side, and towards north-east for the east side.

4. Wave Energy Converters

4.1. Technologies

To select the best converter for the Caspian Sea wave energy recovery, a variety of wave energy converters are evaluated in the next section. There are currently about 80 technologies for wave energy conversion. Wave energy converter systems can be categorized into four main categories, including wave-activated bodies, point absorbers, oscillating wave columns and overtopping systems. These categorizations are based on installation and deployment on shoreline, offshore, or on the sea bed and a brief description of each provided in this subsection [38–41].

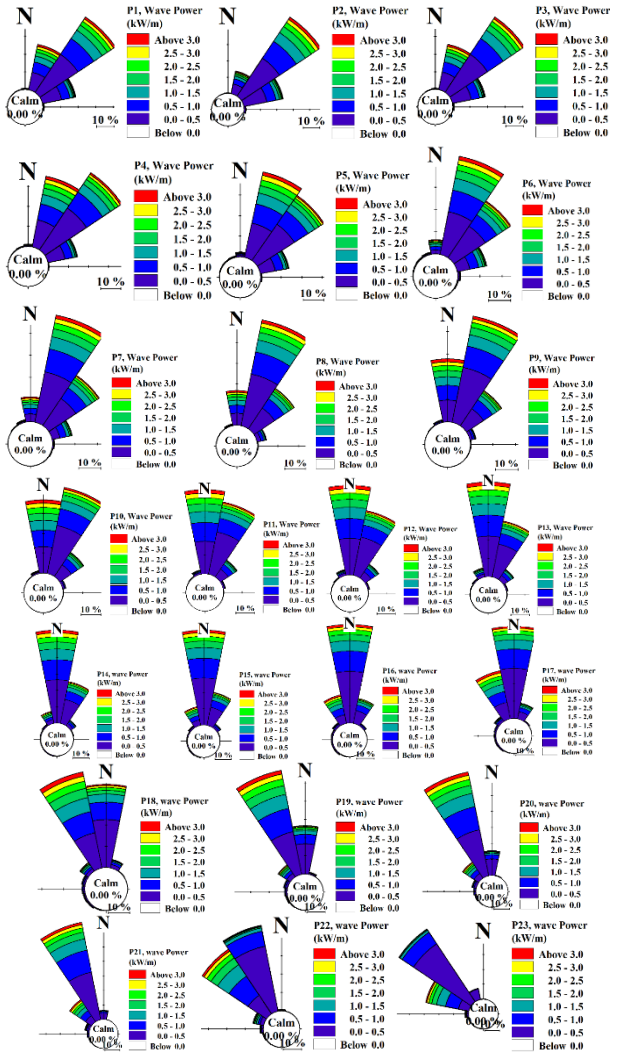

Figure 8. wave rose diagrams from the fifteen-years modeling

Active devices operate by moving relative oscillation bodies from the wave motion. These devices include an unbreakable reference that the absorbing body can fluctuate towards, and the energy is constrained by the power transmission system via dipping or resisting

movement of these objects. The converters are Pelamis [42], DEXA [43], WEPTOS [44], Anaconda [45], SEAREV [46], Salter Duck [47], McCabe [48], WaveRoller [49], Oyster [50], and BioWave [51], the characteristics of which are given in Table 4.

Table 4. Characteristics of WAB devices

Device	Type	Water Depth (m)	Average Wave Power (KW/m)	Output Power (kW)
Pelamis	Floating on sea surface	50	40-70	750-2250
DEXA	Floating on sea surface	50	10	160
WEPTOS	Fixed on sea surface	16.3	39	925
Anaconda	Floating on sea surface	75	50	1000
SEAREV	Fixed on sea surface	50	40	500
Salter Duck	Floating on sea surface	2-30	24	375
McCabe	Floating on sea surface	30-40	53	257
WaveRoller	Fixed on sea coast	10-15	40	300
Oyster	Fixed on seabed	20	19	200
BioWave	Fixed on seabed	25-40	35-50	250

4.1.2 Point Absorbers

Point absorbers are devices that move their relative oscillation bodies via wave motion. These devices include an unbreakable reference that the absorbing body can fluctuate towards, and the energy is constrained by the power transmission system by dipping or resisting movement of these objects. OPT Power [52], AquaBuoy [53], WaveBob [54] and Archimedes Wave Swing [55] are of a variety of converters, and their characteristics are described in Table 5.

Table 5. Characteristics of Point Absorber devices

Device	Type	Water Depth (m)	Average Wave Power (KW/m)	Output Power (kW)
OPT Power	Floating on sea surface	30-60	50	40-500
AquaBuoy	Fixed on sea surface	45-76	20-50	250
WaveBob	Fixed on sea surface	21-24	70-80	131
Archimedes Wave Swing	Fixed on seabed	43	30-40	221

4.1.3. Oscillating Water Column (OWC)

Oscillating Water Column is an offshore deep water converter which compresses the air above the surface of the water and the swells cause the water column to force the air through an air turbine, resulting in the movement of the turbine. This method is considered to be the most efficient method, since its efficiency is about 80% with a relatively simple mechanism and is resistant to storms. The characteristics of these converters can be found in Table 6 which include OSPREY [56], Limpet [57], Mutriku [58] and Mighty Whale [59].

Table 6. Characteristics of OWC devices

Device	Type	Water Depth (m)	Average Wave Power (KW/m)	Output Power (kW)
OSPREY	Floating on sea surface	14.5	50	500
Limpet	Fixed on coast	6	20	113
Mutriku	Fixed on coast	5	26	68.5
Mighty Whale	Fixed on sea surface	40	15	110

4.1.4. Overtopping Devices

These systems are partly dipped in water, which uses wave energy to transfer seawater into a sloping canal and fill a reservoir. Using the height difference, low height turbines move and generate energy. The characteristics of Wave Dragon [60], Tapchan [61] and Sea Slot-Cone Generator (SSG) [62] are described in Table 7.

Table 7. Characteristics of Overtopping devices

Device	Type	Water Depth (m)	Average Wave Power (KW/m)	Output Power (kW)
Wave Dragon	Fixed on sea surface	20-40	60	625-940
TAPCHAN	Fixed on coast	20	20-30	350
SSG	Fixed on coast	6-18	14-16	49-62

4.2. WEC Selection Framework

The factors affecting the selection of a wave energy converter in the Caspian Sea are divided into two main parts; the first part is related to the physical conditions associated with the Caspian Sea, and the second part is related to the structural properties of the wave power converter. Having considered all these criterions, the most suitable energy converter for Caspian sea is selected.

- **Wave energy potential:** As shown in Figures 7 and 8, the waves of the Caspian Sea have a characteristic wave height of 0 to 2 meters and a potential power average of 1 to 4 kilowatt-per-meter near the coast.
- **The converters power output:** The amount of power generated by a device that is normalized according to mass, volume, and capital cost. This factor is the most important decision making parameter. Each wave power converter

system is rated on a scale of 1 and 10 points based on its power generation potential.

- **Sea-bed conditions:** Wave energy converters that are hooked to the seabed cannot be deployed in the Caspian Sea due to its relatively unstable seabed. Hence we assign a score of 1 for systems that are fixed onto the seabed, a Score 4 for systems that are fixed on the shore, a score of 7 for systems floating on the surface of the water, and a score of 10 for converters that do operations without need of seabed.
- **The development of wave power converter devices:** Wave energy converters vary in terms of technology advancements and development. Figure 9 depicts the share of each technology in worldwide wave power generation [24]. Therefore, score 10 for point absorber buoy converters, 6 for WABs, 3 OWCs, and 2 scores for overtopping converters are assigned, respectively.

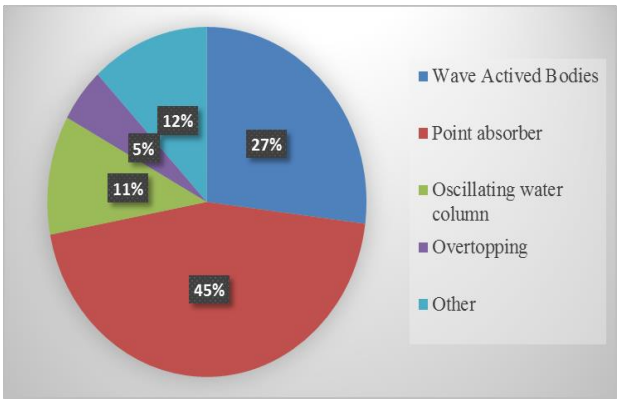

Figure 9. The share of each WEC in the worldwide wave power generation [24]

Based on the above factors, the specific scores for each technology of the available wave energy converters are given in Table 8 based on which the total score of each device is calculated and shown in Figure 10. As it can be seen, the best technology to harness energy in the Caspian Sea is the WEPTOS device which benefits from low complexity while offering high efficiency.

Table 8. Related parameter scores for wave energy absorbers to be used in Caspian sea

Device	Device Progress	Sea Condition	Power
Pelamis	6	7	10
DEXA	6	7	6
WEPTOS	6	10	9
Anaconda	6	7	7
SEAREV	6	10	5
Salter Duck	6	7	6
McCabe	6	7	2
WaveRoller	6	4	3
Oyster	6	1	4
BioWave	6	1	2
OPT Power	10	7	2
AquaBuoy	10	10	3
WaveBob	10	10	1
Archimedes Wave Swing	10	1	2
OSPREY	3	7	4
Limpet	3	4	2
Mutriku	3	4	1
Mighty Whale	3	10	3
Wave Dragon	2	7	7
TAPCHAN	2	4	5
SSG	2	4	2

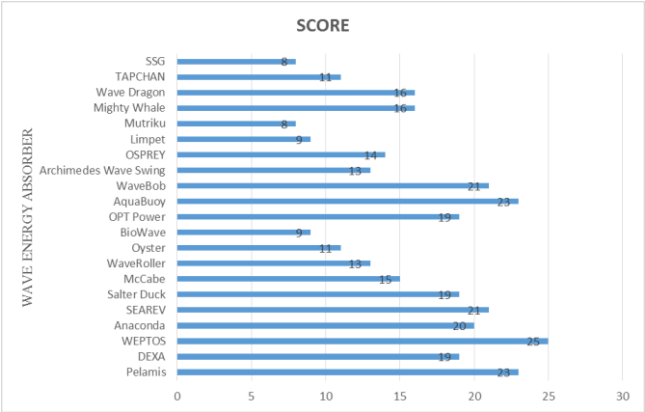

Figure 10. Evaluation of the wave energy absorbers

The structural shape of the WEPTOS device is similar to the letter A. This converter is comprised of two symmetrical arms, each of which consists of 20 separate rotors [63]. The rotors on each arm are connected to a separate generator. The transfer of torque from arm to the generator is carried out through a gear mechanism. The angle of the arms varies depending on the weather conditions. In less extreme near shore climates, the arm length increases in order to harvest the maximum wave energy from a wide range of ocean waves. This enhances the energy produced and covers a wider range of waves, which significantly increases the average annual energy received from the waves. Furthermore, in extreme storm condition, the angle between the arms decreases to prevent structure damage due to the force applied through the waves. In such a situation, minimizing cross-sectional area of the device exposed to the waves, the maximum force from the maximum force applied to the device in the normal state does not exceed. This device has the following distinctive features that distinguish it from other converters [64]:

- High efficiency
- Low capital cost
- Scalability of the device (depending on the conditions, adding or lowering the rotor modules can reduce or increase the capacity of the converter)
- Suitable for low height of waves (for example, for waves with Hs between 0 and 3 meters and Tp between 3 and 7 seconds [44])

5. Conclusions

This study aimed to investigate the potential of wave energy in the Caspian Sea from the Iranian perspective, as a baseline for a framework to select an absorber to harvest this energy. To this aim, the wave power potential was evaluated using the 15-year period annual, seasonal, and monthly wind data from ECMWF for 23 selected stations on the southern side of the Caspian Sea. Furthermore, these results, from the simulation performed by MIKE, were validated based on real data for two stations, including the Anzali and The Neka stations. The error measurement factors such as RMSE and BIAS factors showed great goodness of fit to simulate the wave energy in the region of the case study.

In the next step, a framework is proposed to select an absorber for harvesting the wave energy on the southern coast of the Caspian Sea based on the results of this phase and the geographical conditions. The results indicate that the best technology to harness energy in the Caspian Sea is the WEPTOS absorber. This technology benefits from low complexity while offering high efficiency.

6. References

[1] S. Foteinis, J. Hancock, N. Mazarakis, T. Tsoutsos, and C. E. Synolakis, "A comparative analysis of wave power in the nearshore by WAM estimates and in-situ (AWAC) measurements. The case study of Varkiza, Athens, Greece," *Energy*, vol. 138, pp. 500–508, Nov. 2017.

[2] "Outlook for Energy: A perspective to 2040 | ExxonMobil." [Online]. Available: https://corporate.exxonmobil.com/Energy-and-environment/Looking-forward/Outlook-for-Energy/Outlook-for-Energy-A-perspective-to-2040#Buildingaperspective. [Accessed: 15-Sep-2020].

[3] S. M. Mortazavi, A. Maleki, and H. Yousefi, "Analysis of robustness of the Chinese economy and energy supply/demand fluctuations," *Int. J. Low-Carbon Technol.*, vol. 14, no. 2, pp. 147–159, 2019.

[4] E. Ahmadi, B. McLellan, S. Ogata, B. Mohammadi-Ivatloo, and T. Tezuka, "An integrated planning framework for sustainable water and energy supply," Sustain., vol. 12, no. 10, 2020.

[5] J. C. S. Barstow, G. Mørk, D. Mollison, "*The Wave Energy Resource*," Ocean wave energy, Springer, pp. 93–132, 2008.

[6] O. Langhamer, K. Haikonen, and J. Sundberg, "Wave power-Sustainable energy or environmentally costly? A review with special emphasis on linear wave energy converters," *Renew. Sustain. Energy Rev.*, vol. 14, no. 4, pp. 1329–1335, 2010.

[7] A. F. de O. Falcão, "Wave energy utilization: A review of the technologies," *Renew. Sustain. Energy Rev.*, vol. 14, no. 3, pp. 899–918, Apr. 2010.

[8] B. Drew, A. R. Plummer, and M. N. Sahinkaya, "A review of wave energy converter technology," vol. 223, pp. 887–902, 2009.

[9] R. Pelc and R. M. Fujita, "Renewable energy from the ocean," *Mar. Policy*, vol. 26, no. 6, pp. 471–479, 2002.

[10] M. Mohammadi, R. Ghasempour, F. Razi Astaraei, E. Ahmadi, A. Aligholian, and A. Toopshekan, "Optimal planning of renewable energy resource for a residential house considering economic and reliability criteria," *Int. J. Electr. Power Energy Syst.*, vol. 96, no. September 2017, pp. 261–273, 2018.

[11] N. Ghorbani, A. Kasaeian, A. Toopshekan, L. Bahrami, and A. Maghami, "Optimizing a hybrid wind-PV-battery system using GA-PSO and MOPSO for reducing cost and increasing reliability," *Energy*, vol. 154, pp. 581–591, 2018.

[12] M. Leijon, H. Bernhoff, M. Berg, and O. Ågren, "Economical considerations of renewable electric energy production—especially development of wave energy," *Renew. Energy*, vol. 28, no. 8, pp. 1201–1209, 2003.

[13] A. Rashid and S. Hasanzadeh, "Status and potentials of offshore wave energy resources in Chahbahar area (NW Omman Sea)," *Renew. Sustain. Energy Rev.*, vol. 15, no. 9, pp. 4876–4883, 2011.

[14] S. M. Mortazavi and S. Garoosi, "Role of Energy Supply and demand Fluctuations in Macroeconomic Development of Iran," vol. 1, no. 1, pp. 85–92, 2019.

[15] S. C. Pryor and R. J. Barthelmie, "Climate change impacts on wind energy: A review," *Renew.*

Sustain. Energy Rev., vol. 14, no. 1, pp. 430–437, 2010.

[16] M. Mehrpooya, M. Mohammadi, and E. Ahmadi, "Techno-economic-environmental study of hybrid power supply system: A case study in Iran," *Sustain. Energy Technol. Assessments*, vol. 25, no. September 2016, pp. 1–10, 2018.

[17] G. Iglesias, M. López, R. Carballo, A. Castro, J. A. Fraguela, and P. Frigaard, "Wave energy potential in Galicia (NW Spain)," *Renew. Energy*, vol. 34, no. 11, pp. 2323–2333, 2009.

[18] M. Bahrami and P. Abbaszadeh, "An overview of renewable energies in Iran," *Renew. Sustain. Energy Rev.*, vol. 24, no. 2013, pp. 198–208, 2013.

[19] M. A. Mustapa, O. B. Yaakob, Y. M. Ahmed, C. K. Rheem, K. K. Koh, and F. A. Adnan, "Wave energy device and breakwater integration: A review," *Renew. Sustain. Energy Rev.*, vol. 77, no. September 2015, pp. 43–58, 2017.

[20] A. Al-Habaibeh, D. Su, J. McCague, and A. Knight, "An innovative approach for energy generation from waves," *Energy Convers. Manag.*, vol. 51, no. 8, pp. 1664–1668, 2010.

[21] F. He, Z. Huang, and A. W. Law, "An experimental study of a floating breakwater with asymmetric pneumatic chambers for wave energy extraction," *Appl. Energy*, vol. 106, pp. 222–231, 2013.

[22] J. M. B. P. Cruz and A. J. N. A. Sarmento, "Sea state characterisation of the test site of an offshore wave energy plant," *Ocean Eng.*, vol. 34, no. 5–6, pp. 763–775, 2007.

[23] J. P. Kofoed, P. Frigaard, E. Friis-Madsen, and H. C. Sørensen, "Prototype testing of the wave energy converter wave dragon," *Renew. Energy*, vol. 31, no. 2, pp. 181–189, Feb. 2006.

[24] I. López, J. Andreu, S. Ceballos, I. Martínez de Alegría, and I. Kortabarria, "Review of wave energy technologies and the necessary power-equipment," *Renew. Sustain. Energy Rev.*, vol. 27, pp. 413–434, Nov. 2013.

[25] D. Khojasteh, D. Khojasteh, R. Kamali, A. Beyene, and G. Iglesias, "Assessment of renewable energy resources in Iran; with a focus on wave and tidal energy," *Renew. Sustain. Energy Rev.*, vol. 81, no. December 2016, pp. 2992–3005, 2018.

[26] S. Hadadpour, A. Etemad-Shahidi, E. Jabbari, and B. Kamranzad, "Wave energy and hot spots in Anzali port," *Energy*, vol. 74, pp. 529–536, 2014.

[27] M. Majidi Nezhad, D. Groppi, and G. Piras, "Nearshore Wave Energy Assessment of Iranian Coastlines," pp. 1–8, 2018.

[28] R. Alamian, R. Shafaghat, S. S. Hosseini, and A. Zainali, "Wave energy potential along the southern coast of the Caspian Sea," *Int. J. Mar. Energy*, vol. 19, pp. 221–234, 2017.

[29] B. Kamranzad, A. Etemad-Shahidi, and V. Chegini, "Sustainability of wave energy resources in southern Caspian Sea," *Energy*, vol. 97, pp. 549–559, 2016.

[30] A. Saket and A. Etemad-Shahidi, "Wave energy potential along the northern coasts of the Gulf of Oman, Iran," *Renew. Energy*, vol. 40, no. 1, pp. 90–97, 2012.

[31] T. Whittaker and M. Folley, "Nearshore oscillating wave surge converters and the development of Oyster," *Philos. Trans. R. Soc. A Math. Phys. Eng. Sci.*, vol. 370, no. 1959, pp. 345–364, 2012.

[32] D. P. Cashman, M. G. Egan, and J. G. Hayes, "Modelling and Analysis of an Offshore Oscillating Water Column Wave Energy Converter," *Measurement*, pp. 1–10, 2009.

[33] L. Wang, A. Kolios, L. Cui, and Q. Sheng, "Flexible multibody dynamics modelling of point-absorber wave energy converters," *Renew. Energy*, vol. 127, pp. 790–801, 2018.

[34] Bevilacqua.G and Zanuttigh.B, "Overtopping Wave Energy Converters : general aspects and stage of development," *Int. Coast. Eng. Proc.*, no. 1, p. 21, 2011.

[35] L. Rusu and C. Guedes Soares, "Wave energy assessments in the Azores islands," *Renew. Energy*, vol. 45, pp. 183–196, 2012.

[36] G. Kim, W. M. Jeong, K. S. Lee, K. Jun, and M. E. Lee, "Offshore and nearshore wave energy assessment around the Korean Peninsula," *Energy*, vol. 36, no. 3, pp. 1460–1469, 2011.

[37] Danish Hydraulic Institute (DHI), "Mike 21 Wave Modelling," *Dhi*, pp. 1–18, 2009.

[38] L. B. M. Andersen M, Argyriadis K, Butterfield S, Fonseca N, Kuroiwa T, "Ocean Wind and Wave Energy Utilization," vol. 2, no. August, 2006.

[39] M. Previsic, "Wave power technologies," Proc. 2005 *Int. Conf. Futur. power Syst. IEEE*, 2005.

[40] S. M. Polinder H, "Wave energy converters and their impact on power systems," *Proc. 2005 Int. Conf. Futur. power Syst.*, pp. 1–9, 2005.

[41] A. Clément et al., "Wave energy in Europe: current status and perspectives," *Renew. Sustain. Energy Rev.*, vol. 6, no. 5, pp. 405–431, 2002.

[42] C. Retzler, "Measurements of the slow drift dynamics of a model Pelamis wave energy converter," *Renew. Energy*, vol. 31, no. 2, pp. 257–269, Feb. 2006.

[43] J. Peter and P. Bak, "Near-Shore Floating Wave Energy Converters," *Coast. Eng.*, 2011.

[44] A. Pecher, J. P. Kofoed, and T. Larsen, "Experimental Study of the Weptos Wave Energy Converter," *31th Int. Conf. Ocean. Offshore Arct. Eng. OMAE*, pp. 1–11, 2012.

[45] V. Heller, J. Chaplin, and F. Farley, "Physical model tests of the anaconda wave energy converter," *Proc. 1st IAHR Eur. Congr.*, vol. 1, pp. 3–8, 2000.

[46] M. Ruellan, H. Ben Ahmed, B. Multon, C. Josset, A. Babarit, and A. H. Clément, "Design Methodology for a SEAREV Wave Energy Converter," *IEEE Trans. Energy Convers.*, vol. 25, no. 3, pp. 760–767, 2010.

[47] S. Duck, "Edinburgh Wave Power Group, Salter Duck." [Online]. Available: http://www.mech.ed.ac.uk/research/wavepower/.

[48] T. W. Thorpe, "A Brief Review of Wave Energy," *Tech. Rep. ETSU-R120*, no. May, p. 200, 1999.

[49] T. Mäki, M. Vuorinen, T. Mucha, and T. Waveroller, "WaveRoller – One of the Leading Technologies for Wave Energy Conversion," *5th Int. Conf. Ocean Energy*, no. November, pp. 4–6, 2014.

[50] T. Whittaker, D. Collier, M. Folley, M. Osterried, and A. Henry, "The development of Oyster - A shallow water surging wave energy converter ," *7th Eur. Wave Tidal Energy Conf.*, no. January 2017, 2007.

[51] F. Zabihian and A. S. Fung, "Review of marine renewable energies: Case study of Iran," *Renew. Sustain. Energy Rev.*, vol. 15, no. 5, pp. 2461–2474, 2011.

[52] B. S. Holmes B, "State of the Art Analysis - A Cautiously Optimistic Review of the Technical Status of Wave Energy Technology," *EU Proj. Rep.*, pp. 1–111, 2009.

[53] M. Previsic, R. Bedard, and G. Hagerman, "E2I EPRI Assessment Offshore Wave Energy Conversion Devices," *E2I EPRI WP – 004 – US – Rev* 1, pp. 1–52, 2004.

[54] J. Weber, F. Mouwen, a. Parish, and D. Robertson, "Wavebob – Research & Development Network and Tools in the Context of Systems Engineering," Ewtec, no. *Proc. of the 8th European Wave and Tidal Energy Conf.*, Uppsala, Sweden, pp. 416–420, 2009.

[55] M. Prado, "Archimedes wave swing (AWS)," *Ocean wave energy, Springer, Berlin*, pp. 297–304, 2008.

[56] J. F. Childs, "THE ROLE OF CONVERTERS & THEIR CONTROL IN THE RECOVERY OF WAVE & WIND ENERGY," *Proc. IEE Colloq. power Electron. Renew. energy*, vol. 43, no. 1, pp. 23–25, 1997.

[57] T. J. T. Whittaker, W. Beattie, M. Folley, C. Boake, a Wright, and M. Osterried, "The Limpet Wave Power Project – The First Years Of Operation," *Scottish Hydraul. Study Gr. - Semin. Hydraul. Asp. Renew. Energy*, no. 1997, pp. 1–8, 2004.

[58] Y. Torre-Enciso, I. Ortubia, L. I. López de Aguileta, and J. Marqués, "Mutriku Wave Power Plant: from the thinking out to the reality," *8th Eur. Wave Tidal Energy Conf.* (EWTEC 2009), pp. 319–328, 2009.

[59] Y. Washio, H. Osawa, and T. Ogata, "The open sea tests of the offshore floating type wave power device 'mighty whale' - Characteristics of wave energy absorption and power generation," *Ocean. Conf. Rec.*, vol. 1, pp. 579–585, 2001.

[60] J. P. Kofoed, P. Frigaard, E. Friis-Madsen, and H. C. Sørensen, "Prototype testing of the wave energy converter wave dragon," *Renew. Energy*, vol. 31, no. 2, pp. 181–189, 2006.

[61] de O. F. A. Evans DV, *Hydrodynamics of ocean wave-energy utilization*. 1985.

[62] D. Vicinanza, L. Margheritini, J. P. Kofoed, and M. Buccino, "The SSG wave energy converter: Performance, status and recent developments," *Energies*, vol. 5, no. 2, pp. 193–226, 2012.

[63] G. Mattiazzo and A. Gulisano, "Wave energy future," 2016.

[64] "WEPTOS Company Website." [Online]. Available: http://www.weptos.com/.